Control of Drug Bioavailability using Hybrid Mesoporous Silica Nanoparticles

Giorgia Figari

Instituto Superior Tecnico, Lisboa , Portugal

December 2020

Abstract

The poor water solubility of many drugs has emerged as one of the major challenges in the pharmaceutical world. Amorphous solid dispersions have been considered as the major advancement in overcoming limited aqueous solubility and oral absorption issues. The main drawback of this approach is that they can lack the necessary stability and revert to the crystalline form on storage. Significant upfront development is therefore, required to generate stable amorphous formulations. The objective of this work is to use mesoporous silica in amorphous oral drug delivery systems. In particular, the aim is to increase the bioavailability of a commercial drug, fenofibrate, by promoting its amorphous state when confined in mesoporous silica nanoparticles (MSNs). MSNs nanovehicles with diameters under 100 nm were functionalized with different organic groups in the pores to tune the interaction of the drug with the matrix and thus avoid its crystallization which impairs bioavailability. This approach has the potential for application in different systems and offers two advantages: (i) provides a vehicle for controlled delivery and (ii) stabilizes the amorphous state, improving the solubility and bioavailability of the drug. The potential advantage of MSNs as inert, hydrophilic, pharmaceutical carrier matrices is discussed. A brief introduction to the Biopharmaceutical Classification System, nanoparticles and the solubility advantage of amorphous drugs is provided. In addition, the preparation, characterization and functionalization of MSNs for drug release are also presented. In the present study fenofibrate was loaded in a silica matrix with and without functionalization of their pores with two modifying agents that differs in hydrophilicity. Specifically, hydrophilic (3-Aminopropyl) triethoxysilane (APTES) and hydrophobic trimethoxy(phenyl)silane (TMPS). To access the physical state of fenofibrate inside the silica matrix, differential scanning calorimetry (DSC) was used. Dielectric relaxation spectroscopy (DRS) was applied to probe the molecular mobility of the drug. The different techniques provided complementary information and reveal that drug incorporation inside a nanoporous matrix is a suitable strategy to stabilize fenofibrate in the amorphous state. Release studies were performed to analyze how the physical state of loaded fenofibrate into bare and functionalized mesoporous silica nanoparticles is reflected in the delivery.

Keywords: mesoporous silica nanoparticles, solubility, amorphous state, drug release, pore functionalization

1. Introduction

The most common route of drug administration is the oral one. However, the major challenge with the design of oral dosage forms lies with the poor bioavailability of many pharmaceutics. The most frequent causes of low oral bioavailability are attributed to poor solubility and low permeability. [1] Solubility is one of the important parameters to achieve desired concentration of drug in systemic circulation for pharmacological response, and consequently it represents a major challenge for formulation. Currently, more than 40% new chemical entities (NCEs) developed in pharmaceutical industry are practically insoluble in water which limits their use. [2] Thus, the solubility problems complicate the delivery of these new drugs and also affects the delivery of many existing drugs. Amidon et al. [3] classified active pharmaceutical ingredients (APIs) into four groups based on their solubility and permeability known as the Biopharmaceutical Classification System (BCS). For instance, BCS class II drugs have low solubility and high permeability, thus, in this case, increasing the solubility should increase the bioavailability. Therefore, there is great interest to develop reliable, efficient, cost effective, and scalable methods to increase the aqueous solubility of BCS class II drugs. Among other strategies, converting crystalline drugs into an amorphous form is one the most promising tool to overcome the problem of poor solubility. The process of amorphization of the drug substance involves disruption of the ordered structure of a crystal which can be achieved by using a process like melt cast, hot melt technology and spray drying. Hence, amorphous drug exists in a higher free energy state and it has higher mobility as compared to its crystalline counterpart. Thus, the thermodynamic properties of amorphous state may result favorable to obtain a higher apparent solubility and dissolution rate. However, due to high internal energy and enhanced molecular mobility, amorphous substances may tend to crystallize

during storage and dissolution. [4]
To benefit from the amorphous state, efforts have been made to reduce the driving force of recrystallization. For example, Beiner et al. [5] and Graubner et al. [6] shown that it is possible to stabilize substances in the amorphous state by incorporating in mesoporous matrix due to the confinement inside the pores that may prevent the rearrangement of the amorphous molecules into long-range order. Moreover, mesoporous silica materials offer several attractive features, which render them excellent candidates for controlled drug delivery systems such as tunable pore size and structure, large surface areas and pore volumes, controllable morphology and modifiable surfaces and high thermal and chemical stabilities. [7] Furthermore, the most remarkable advantage of MSNs materials as drug delivery systems is their "zero premature controlled release" property. Namely, drugs are carried with precise control of location and time without leaching prior to reaching the targeted cells or tissues and this will reduce drug dosage and side effects. [8]
First synthesized by Mobil corporation scientists in 1992 [9], these MSNs are composed by an amorphous matrix of silica (SiO_2) with nanometric size pores ordered in different arrangements, depending on the synthesis process. However, it is a challenge to find a simple, sustainable, and scalable synthetic process to tune their diameter in the range of a few tens of nanometers, with narrow size dispersity. [10]
Generally, a modified Stober 'sol-gel process' is used to produce MSNs with controlled mesopore structure and surface properties. The sol-gel process involves the hydrolysis and condensation of the alkoxide monomers into a colloidal solution (sol), which acts as a precursor to form an ordered network (gel) of discrete particles in basic medium. [11] The most commonly silica alkoxide is tetraethyl orthosilicate (TEOS). The mechanism of MSNs preparation relies on the use of a template (usually a surfactant, such as CTAB) which above the critical micellar concentration forms cylindrical micelles that aggregate to form the mesoporous structure in the silica nanoparticles.
After hydrolysis of the silicon alkoxide, condensation occurs around the micellar aggregates. The subsequent removal of the templates originates mesoporous silica nanoparticles with free pore available for the incorporation of molecules (Figure 1). These nanoparticles are biocompatible and the three-dimensional network with silanol groups (= Si-OH) inside the pores or on the surface, and siloxane (= Si-O-Si =) inside the network, attribute the hydrophilic characteristic to the particles. [8]

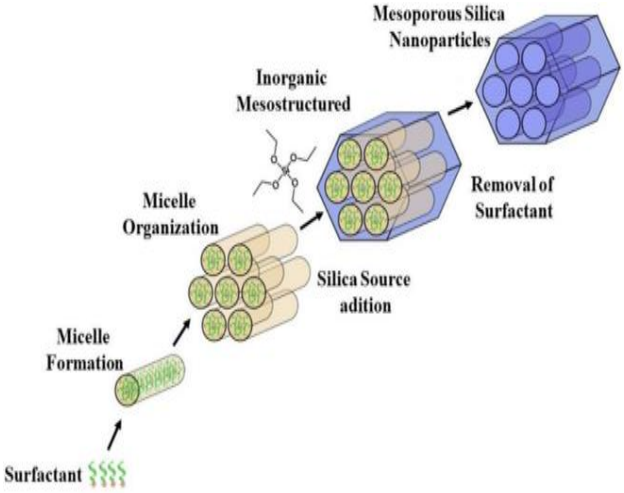

Figure 1. Illustration of mesoporous material formation with surfactant adapted from [12]).

MSNs have two functional surfaces, the outer surface of the particles and the pore channels. This feature allows both surfaces to be selectively functionalized. There are two different approaches, either by co-condensation or by post synthetic methods [13]. The most common process of nanoparticles functionalization is by post synthesis modification (also known as grafting). This method can be performed either before or after the template removal. However it has the disadvantage that it can be difficult to achieve a homogeneous distribution of the organic group due to the fact that major functionalization reactions take place between organic precursors and free silanol groups at the exterior surface and at the opening of the pores of MSNs. [14] The co-condensation method consists in introducing organ silanes simultaneously with silica precursors during the synthesis of MSNs materials. Thus, by applying this method it is possible to obtain a more homogeneous distribution of the functional groups as they are components of the silica network [15] and it is also possible to control mesoporous silica nanoparticle morphology by the introduction of different organ silanes that will interact in a different manner with the surfactant molecules. [16]
Lin and coworkers [13] demonstrated that organosilanes with hydrophobic groups tend to intercalate their organic groups into the surfactant micelles and interact with the hydrophobic tails of surfactants, thus stabilizing the formation of long cylindrical micelles and giving rise to rod-shaped MSNs materials. However, the organic group can also destabilize the micelles during the formation of MSNs if the functional group is more hydrophilic, since surfactant interaction with polar group are not favored because they inhibit micelle growth and yield spherical particles with randomly oriented

pore structures. [13] The main objective of this work consists in the synthesis of mesoporous silica particles with pore diameter in the nanometer scale. In a second step, the pore surface will be modified with two different groups in order to tune the interaction of the drug within the matrix and thus stabilizes a BCS class II drug, fenofibrate, in its amorphous state which may lead to an increase in its solubility.

2. Experimental Part

2.1. Materials

Absolute ethanol (EtOH, >99.9% Scharlau), tetraethoxysilane (TEOS, ≥99%, Aldrich), cetyltrimethylammonium bromide (CTAB, ≥99%, Sigma) and sodium hydroxide solution (NaOH 1,4 M) were used without any purification in the synthesis of mesoporous silica nanoparticles. For the removal of the surfactant a solution of 0.5M hydrochloric acid (HCl, 37% Panreac) in absolute ethanol was used. The deionized water was produced from a Millipore system Milli-Q ≥18 MΩcm (with a Millipak membrane filter 0.22 μm). Regarding nanoparticles functionalization, they were surface modified with phenyltrimethoxysilane (97% TMPS, Sigma Aldrich) and (3-Aminopropyl) triethoxysilane (98% APTES, Sigma-Aldrich) without any treatment in dried toluene which was distilled over calcium hydride before use. For NMR analysis samples was used 1,3,5-trioxane (≥99.0%, Fluka), deuterium oxide (D_2O, 99.9% atom, CIL) and dimethyl sulfoxide D6 (DMSO, 99,9%, CIL). disodium hydrogen phosphate (NaH_2PO_4, 99%, Riedel-de-Haën) and sodium dihydrogen phosphate monohydrate ($NaH_2PO_4.H_2O$, 98%, Panreac) were used to prepare the phosphate buffer solution (PBS, pH 8) for the release studies. The cargo molecule used in the studies was Fenofibrate (CAS number 49562-28-9, purchased from Sigma-Aldrich (purity ≥ 99 %) and it was used without further purification. The empirical formula is $C_{20}H_{21}O_4Cl$ and the molecular weight is 360.83 g/mol. The chemical structure is presented in figure 2.

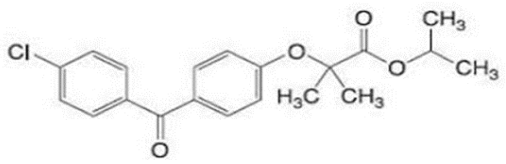

Figure 2. Structure of fenofibrate (FNB).

2.2. Equipment

The nanoparticles were characterized by TEM. TEM images were obtained on a Hitachi transmission electron microscope (Hitachi High – technologies, Tokyo, Japan), model H-8100, with a LaB6 filament (Hitachi) with an accelerator voltage of 200 kV. A camera KeenView (Soft Imaging System, Münster, Germany) is incorporated in this equipment, which through iTEM software, allows acquiring TEM images. MSNs dispersed in ethanol were prepared and dried on a copper grid coated with carbon. The size/dimension, polydispersity, and morphology of the particles were estimated by evaluating at least 50 nanoparticles by Image J software. Fourier Transform Infrared Spectroscopy (FTIR) spectra of pure organosilanes and functionalized MSNs were collected on a Bruker (model: Alpha) over the range 400-4000 cm^{-1} at room temperature. The samples were properly mixed with potassium bromide (KBr) in a mortare and pestle to form homogeneous mixture and punched using a KBr press.

^{1}H-NMR quantification was obtained on an AMX-400 instrument (Bruker, MA, USA). The thermal features were examined using differential scanning calorimeter DSC Q2000 from TA Instruments Inc. (Tzero DSC technology) operating in the Heat Flow T4P option. Enthalpy (cell constant) and temperature calibration were based on the melting peak of indium standard (T_m=156.60 °C). Approximately 5 mg of each sample were introduced in an aluminum hermetic pans with a Tzero hermetic lid with a pinhole to facilitate the exit of water. Thermograms of all the samples were obtained over a range of -90°C to 120°C at a heating rate of 10°C/min under a nitrogen flow of 50 mL/min and they were analyzed during heating. Then, the analysis of data was carried out using the software Universal Analysis 2000 from Thermal Analysis. Melting point (T_m) was determined as the minimum of the endothermic peak, whereas glass transition temperature (T_g) was determined at the onset of the glass transition. Dielectric measurements were carried out using the ALPHA-N impedance analyzer from Novocontrol Technologies GmbH, covering a frequency range from 0.1 Hz to 1 MHz. The sample powder was placed between two gold-plated electrodes of a parallel plate capacitor, BDS 1200 with two 50 μm-thick silica spacers. The sample cell was mounted on a BDS 1100 cryostat and exposed to a heated gas stream being evaporated from a liquid nitrogen dewar. The temperature was controlled by Quatro Cryosystem and performed within 0.5 K. The dielectric relaxation spectra were collected on heating from -150°C up to 150°C regarding the unloaded nanoparticles and up to 120°C for samples with fenofibrate in order to avoid degradation of the drug. Temperature was increased in different steps: from – 150°C to 50°C in steps of 5°C and in the remaining temperature range, every 2°C. The efficiency of loading and the FNB release were studied by UV-VIS spectroscopy. For the absorbance spectra was

used a V-660 UV-Vis spectrophotometer from Jasco International (Tokyo, Japan) with a double monochromator and photomultiplier tube detector for high resolution. The measurements were carried out in quartz cells (with dimensions of 1 cm x 1 cm) at 25°C and using a polypropylene dialysis device with a cellulose membrane (Slide-A-Lyzer Mini Dialysis Devices, 10K MWCO, 0.5 mL) in the release studies. For the release studies 1.73 mg of FNB@MSNs_APTES and 1.63 mg of FNB@MSNs_TMPS were placed in the dialysis membrane with a solution of PBS/EtOH(10%).
The MSNs centrifugations were carried out on an Avanti J-301 (Beckman Coulter) for cleaning bare MSNs after template removal. A Sigma 2k15 (B. Braun) centrifuge, rotor 12141, was used for washing functionalized MSNs at 1100 min^{-1} and a Hitachi Himac CT 15RE was utilized for washing bare and functionalized nanoparticles after drug loading at 150 rpm.

2.3. Methods

2.3.1. MSNs Synthesis

Silica mesoporous nanoparticles (MSNs) were synthesized by the sol-gel method. In a polypropylene flask with flat bottom 1.75 mL NaOH 1.4 M and 240 mL H_2O milli-Q were mixed. The mixture was transferred in an oil bath and heated to 32°C.The reaction was done in homogeneous stirring in order to have a stable mixture and avoid a larger distribution of diameters. Afterwards, 500 mg of CTAB were added to the solution and maintained under stirring for 30 min. Then, 2.5 ml of TEOS were added, drop by drop, and the solution was kept under continuous stirring for 3h at 35°C. The solution turned opaque almost immediately, indicating that the reaction has started. After cooling, the dispersion was put in polypropylene tubes with a capacity of 50 mL and centrifuged at 30000 G (Sigma 2k15 centrifuge, rotor 12141) for 15 minutes. Subsequently, the MSNs were washed 3 times with a solution of ethanol and water (50% V/V) to remove the excess of CTAB in the surface and in solution. The nanoparticles were dried in the oven at 50°C overnight. Then, 0.5 M HCl\ethanol (25 ml per 500 mg of MSNs) was added to solubilize the CTAB and the solution was sonicated for 15 minutes and left overnight stirring at 50°C. After the 24 hours the particles were washed 3 times. The first wash was done with a solution of ethanol and water (50% V/V) and the second and third with absolute ethanol. Finally, the nanoparticles were left drying overnight in a ventilated oven at 50°C.

2.3.2. Modification of the MSNs Pores

The external and internal surface of MSNs was modified by post synthetic method with organic alkosilanes containing functional groups with different polarity in order to test interactions between the functional groups and FNB. [17].
trimethoxy(phenyl)silane, further mentioned as TMPS and (3-Aminopropyl) triethoxysilane further mentioned as APTES were selected by its hydrophobic and hydrophilic characteristic respectively. The modification of the MSNs surface was performed by suspending the nanoparticles in anhydrous toluene under an argon atmosphere. Then, this solution was sonicated under argon atmosphere for 15 min. Subsequently the alkosilane was added dropwise and the resulting mixture was maintained at 130°C under reflux in an argon atmosphere for 24 h. Quantities are indicated in Table 1. The nanoparticles were recovered by centrifugation and washed three times with ethanol (11000 min^{-1}, 10 minutes), discarding each time the supernatant. After the last centrifugation the particles were left drying at 50°C overnight in a ventilated oven and a solid product was obtained as powder (MSNs_APTES or MSNs_TMPS).

Table 1. Volumes of functionalization compound used in MSNs surface modification

Sample	MSNs (g)	V (mL)
APTES	0.166	0.10
TMPS	0.169	0.05

2.3.3. FNB Loading in MSNs and Modified MSNs

Drug loading of FNB, in bare MSNs and modified MSNs, was performed in solution under vacuum. First MSNs were placed in a glass cell under vacuum (10^{-4} bar) and heated up to 150°C by immersion of the cell in an oil bath for 8 h. After this period, the cell was allowed to cool down and a solution of FNB in 2 mL of acetone was injected in the cell containing the nanoparticles under vacuum and stirred for 3 hours. Finally, the solvent was allowed to evaporate for one day under gentle stirring at room temperature without vacuum, after which a dry powder was obtained (FNB@MSNs or FNB@MSNs_APTES or FNB@MSNs_TMPS). In Table 2 are presented the drug loading conditions for all the silica carriers.

Table·2.·Drug·loading·conditions¶

Sample¤	m_{MSNs} (mg)¤	m_{FNB} (mg)¤	wt%·¤
MSNs¤	140.3¤	41.4¤	22.8¤
MSNs_APTES¤	142¤	42¤	22.8¤
MSNs_TMPS¤	120¤	60¤	33.3¤

3. Results and Discussion

3.1. MSNs Characterization

The morphological evaluation of the MSNs was performed by TEM. The estimated average diameter was 49± 6.6 nm obtained by the analysis of fifty particles in TEM images using ImageJ software. Mesoporous nanoparticles present smooth surface and spherical shape.
Figure 3 shows a TEM image of the synthesized MSNs.

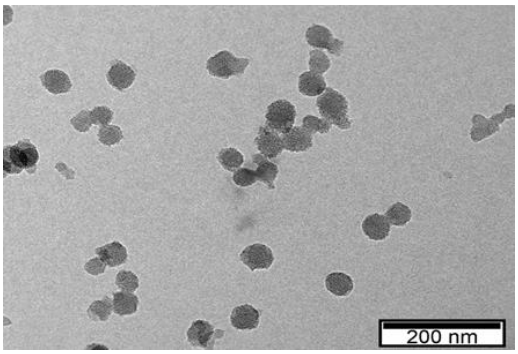

Figure 3. TEM of the synthesized MSNs.

3.2. Identification of Functional Groups by FTIR

The modification on the nanoparticle surface was confirmed by comparing the specific bands of the pure modifying agent with those observed in the functionalized silica. The FTIR spectra collected between 400 and 5000 cm^{-1} are presented in **Errore. L'origine riferimento non è stata trovata.** for pure modifying agent, bare MSNs and modified MSNs. Silica and modified silica samples have strong bands located at around 460 ($\delta_{O\text{-}Si\text{-}O}$), 1100 ($\upsilon_{asym.Si\text{-}O\text{-}Si}$), and 3300-3500 cm^{-1} ($\upsilon_{Si\text{-}OH}$), confirming the presence of SiO2 inorganic phase. [18, 19]
The modified MSNs_APTES show two bands different from unmodified ones (see vertical dot lines in figure 4)

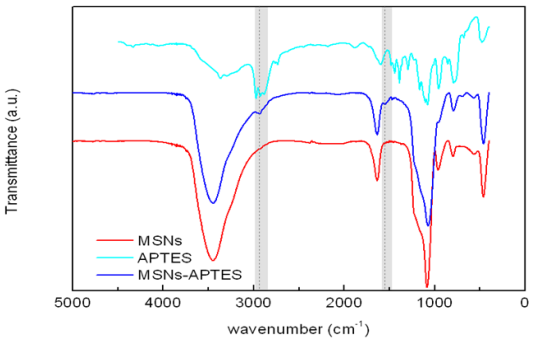

Figure 4. FTIR spectra of pure APTES, bare MSNs and APTES modified MSNs_APTES

Around 2938 cm^{-1} attributed to C-N stretching vibration at 1554 cm^{-1}, related to NH bending vibrations. [19]
These characteristics bands, observed in the FTIR spectra of MSNs_APTES but not in bare MSNs, confirming that the amino-propyl groups of APTES were successfully incorporated in the MSNs. The silica functionalization with TMPS showed the following bands (grey regions in figure 5): Between 2925 cm^{-1} and 2855 cm^{-1} attributed to methoxy groups [20]. At 1433 cm^{-1} attributed to Si-OCH_3 bond [21] . and at 749 cm^{-1} and 700 cm^{-1} attributed to Ph-Si bond [21]

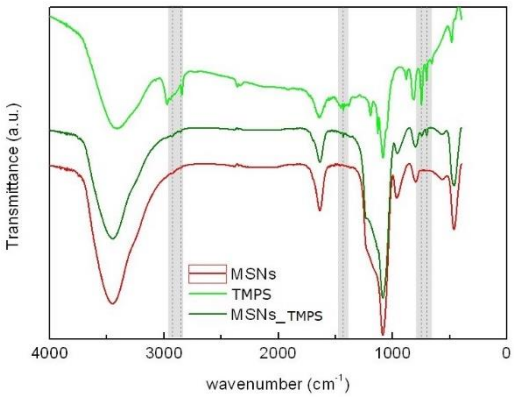

Figure 5. FTIR spectra of pure functionalized agent (TMPS), bare mesoporous nanoparticles (MSNs) and modified mesoporous nanoparticles (MSNs_TMPS).

3.3. Quantification of Functional Groups by ^{1}H NMR

The quantification was carried out via ^{1}H NMR as described by Crucho et al. [22]. This method destroys the nanoparticles and requires an internal standard, such as trioxane, to be used in the quantification. In all the samples, the ethoxy group generates distinct resonance at 1.2 ppm and 3.6 ppm. These peaks correspond to resonances of residual ethanol from washing the MSNs after synthesis (solvent remain entrapped on the silica matrix after drying) and could denote a possible incomplete condensation of the alkoxysilane groups on the MSNs. Concerning MSNs_APTES compound, the amount of the organic molecules grafted on the surface and inside the pores of the MSNs was estimated by comparing the integrated intensities of the peaks from the alpha-carbon to the silicon atom (less affected by possible interactions of the functional group) with the intensity of the internal standard. [20] In figure 6 is presented the ^{1}H NMR spectra for silica nanoparticles functionalized with APTES.

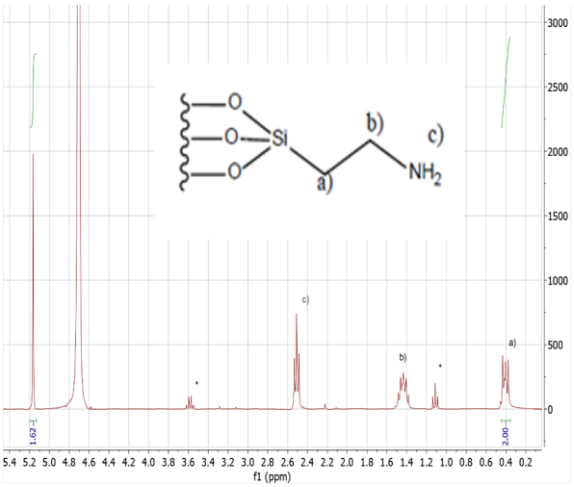

Figure 6. ^{1}H NMR spectra recorded of MSNs_APTES in NaOH/D_2O. The internal standard peak is at 5.15 ppm. Ethanol peaks are marked with (*).

^{1}H NMR (D_2O): 0.38 ppm (t, 2H, Si-CH_2-); 1.41 ppm (q, 2H, -CH_2-); 2.49 ppm (t, 2H, -NH_2); 1.09 ppm (solvent, C**H**$_3$C**H**$_2$OH); 3.57 ppm (solvent, CH_3C**H**$_2$OH); 4.71 ppm (D_2O); 5.15 ppm (internal standard, C_3**H**$_6O_3$). [21]

The results obtained are presented in Table 3 for both the organic molecules used.

Table 3. APTES and TMPS concentrations on the MSNs, calculated by ^{1}H NMR

Sample	mmol/g MSNs	Modifying agent molecules/nm^2
MSNs_APTES	3.14	1.93
MSNs_TMPS	0.98	0.60

Assuming that the three alkoxide groups in an organosilane molecules could covalently react with up to three Si-OH sites, the maximum number of functional groups that can be anchored in the MSNs should be in the range of 1~3 molecules/nm^2. In particular, the values obtained by solution ^{1}H-NMR related to the anchoring of APTES molecules are in good agreement with this upper limit, showing good control of the surface modification procedure.

3.3.1. Identification of FNB in the silicas by FTIR

In a general way, the presence of FNB in the loaded nanoparticles is noted by the several and small intense bands superimposed to the unloaded matrixes. For a more detailed comparison in figure 7 is presented an enlarged portion of FTIR spectra of FNB in all the composites.

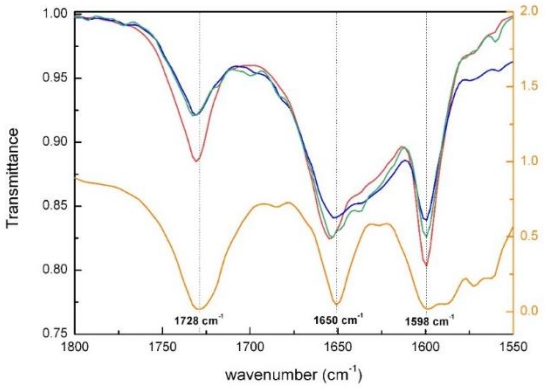

Figure 7. FTIR spectra of bulk FNB (orange) FNB@MSNs (red), FNB@MSNs_APTES (blue) and FNB@MSNs_TMPS (green) in the carbonyl stretching region.

Between 1800 and 1550 cm^{-1} the most relevant bands are: at 1728 cm^{-1} and 1650 cm^{-1} in pure crystalline FNB assigned to stretching vibrations of carbonyl in the ester group and to the carbonyl in the ether group between benzene rings respectively. [23] In FNB loaded these bands are slightly shifted to higher wavenumbers probably due to the amorphization of FNB when it is incorporated inside silicas. Between 1598 and 1570 cm^{-1}, multiple peaks arise partially overlapped in pure FNB which have been assigned to in-plane benzene stretch and benzene ring deformation.[23] When FNB is loaded in mesoporous matrixes, only a very well-defined band is observed in this region, centered at 1600 cm^{-1} (figure 7). This may indicate that only one of the vibration modes, that corresponding to in-plane benzene ring stretch [23], is allowed when FNB is loaded in MSNs. A possible explanation for this effect can be related to the hydrogen bonds formed between FNB and silica. In this sense, it must be noted that FNB can't form hydrogen bonds to other FNB molecules due to the lack of hydrogen-bond donating groups.[23] The disappearance of some of vibration modes could be due precisely to the formation of strong H-bonds between FNB and silica that favor one of the possible stretch vibrations in detriment of the others.

3.4. Physical State of FNB in the MSNs

3.4.1. DSC Results

Differential scanning calorimetry was used to study phase transformations of fenofibrate and fenofibrate incorporated in bare and functionalized silicas. Thermogram of bulk FNB is shown in figure 8.

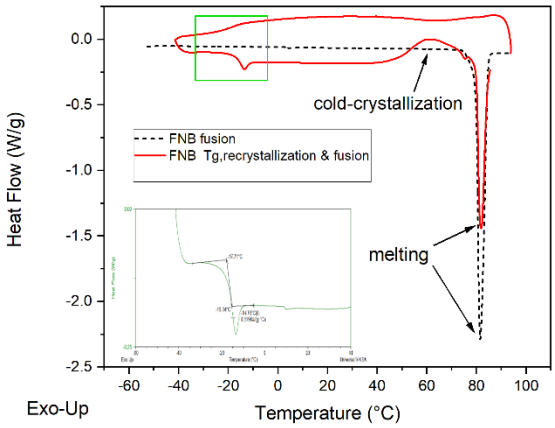

Figure 8. Thermograms of fenofibrate obtained at 10 °C/min: dotted line, on heating from room temperature up to 95°C; red line, upon cooling down to -50°C and then heating up to 90°C. Green square indicates the glass transition region. Data provided by [24].

On heating, FNB melt at 81°C (dotted line) with an enthalpy of 32.4 kJ/mol. On cooling after melting (red line), crystallization is avoided, and it enters in the supercooled liquid state. Around -17°C the signal of the glass transition is observed also in very good agreement with the value obtained.[25] In the subsequent heating, the glass transition temperature can be well defined at -17.71°C ($T_{g\text{-onset}}$). Additionally, a broad exothermic peak was observed which revealed crystallization from the amorphous phase (T_{max} = 63°C). The corresponding melting is found at 81 °C. Given that the temperature is equal to that obtained for the native sample, it can be assumed that the same crystalline and more stable form was originated. The enthalpy of 22.87 J/g indicates that only a fraction of the sample was recrystallized ($\Delta H_{cold\text{-}crystll}/\Delta H_{initial}$ *100 = 25.4 % crystallinity). This indicates that although fenofibrate is a good glass former it has tendency to recrystallize to its stable and structurally ordered crystalline state. Thus, fenofibrate was incorporated into mesoporous matrices with the aim to stabilize the compound in its amorphous form and thus improve its solubility, which may enhance bioavailability. Thermograms of FNB loaded in silica matrixes (functionalized and not) were acquired by a gradual drying treatment consisting in successive cooling/heating cycles with increasing final temperatures in order to better visualize the signal of the glass transition temperature by gradual removing the water that is normally adsorbed into the silicas (found in higher amount in MSNs_APTES).

Besides the glass transition, no signal of thermal events was detected during all the cycles in all the composites even above the melting temperature of fenofibrate meaning that FNB coverts to the amorphous form when is located inside the silica carrier and conversion in its crystalline form is avoided. Moreover, the absence of a melting peak indicates that all the amount of FNB used was successfully incorporated inside the pores of the silicas. The interval of glass transition temperature was defined by the onset of T_g in all the analysis and results had shown lower $T_{g\text{-onset}}$ values of FNB constricted into silicas compare to the one of bulk FNB (T_g= -17.7 °C) values probably due to some plastificant effect of the water. Moreover, being the $T_{g\text{-onset}}$ still below 25°C in all the composites, FNB is in its amorphous state inside the pores in the supercooled liquid state.

3.4.2 DRS Results

Dielectric relaxation spectroscopy (DRS) was used as an excellent technique to probe the molecular mobility of the guest and to access the time scales of the relaxation processes. Figure 9 shows the dielectric modulus of fenofibrate in MSNs at the frequency of 10^5 Hz during first and second heating. Data of native amorphous FNB has been included for comparison. In the spectra of native fenofibrate around 50°C a sharp decrease appears due to the recrystallization followed by a sharp increase some degrees above that corresponds to the melting of the crystal formed. Thus, DRS spectroscopy again leads to confirm that bulk amorphous fenofibrate is not stable and it has tendency to recrystallize. On the other hand, no signal of melting is observed when is loaded in mesoporous silica nanoparticles, in accordance with thermograms obtained by DSC.

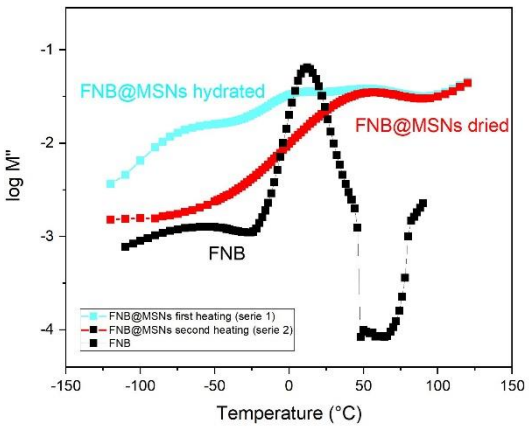

Figure 9. Isochronal representation of M´´ *vs.* T at 10^5 Hz for native FNB (black squares), FNB@MSNs series 1 (hydrated) in light blue, and series 2 (dried) in red.

Subsequently, the mobility of the amorphous fenofibrate into the silicas was analyzed taking data from the dehydrated state named as serie 2. Figure 10 shows the isochronal plots of M´´ for all the frequencies available from 0.1 Hz to 10^6 Hz and from temperatures between -120 and 120°C.

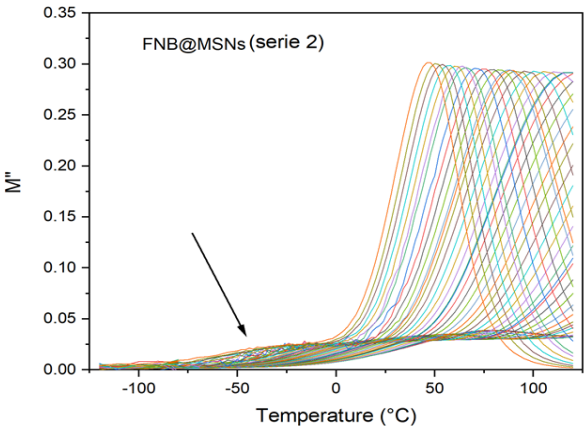

Figure 10. Isochronal representation of M´´ collected in the isothermal mode for the sample FNB@MSNs during the second heating (serie 2). The arrow indicates the relaxation process of constrained FNB under study.

To better investigate the dynamic behavior of fenofibrate in bare and functionalized silica nanoparticles, peaks observed in the isochronal representation of M´´ have been individually analyzed by fitting with gaussian functions. From this analysis, for each frequency it has been estimated the temperature position of each peak observed, *i.e.* pairs as (f, T_{max}). The relaxation time characteristic of each process depends on the mobility of the molecules (dipoles) and it was calculated as $\tau_{max} = 1/2\pi f$.

Then, its temperature dependence has been represented in the relaxation map, -log(τ_{max}) *vs.* 1000/T), that is plotted in figure 11.

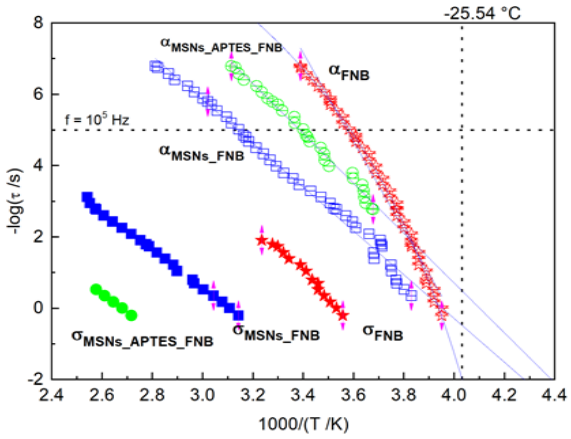

Figure 11. Temperature dependence of the relaxation times of each process observed for FNB@MSNs and FNB@MSNs_APTES in serie 2. Solid lines correspond to the respective Arrhenius and VFTH curve fits. Vertical dot line indicates the T_g extrapolated for amorphous FNB and the horizontal dot line shows a fix frequency for better comparison.

In bulk amorphous FNB (red stars), in the temperature analyzed, two processes were detected, one of them related to the glass transition designated as α process [26] and the other one, at highest temperatures, related to conductivity, (σ, translational motion of charges). Concerning the α, the relaxation time follows a curvature in -logτ *vs.* 1000/T that can be described by the empirical VFTH (Vogel Fulcher Tamman Hess [27]) equation:

$$\tau(T) = \tau_\infty e^{\frac{B}{T-T0}} \qquad \text{(Equation 1)}$$

with parameters B=1722.08 K, T_0=204.8 K and $\tau\infty = 10^{-15.01}$ s.
The glass transition temperature was estimated from dielectric date by extrapolate the fitted curve at τ=100 s and the activation energy associate to this mechanism gives a value of 463 kJ/mol not far from the data reported in reference [23] obtained with other techniques. On the other hand, the relaxation mechanisms observed in FNB loaded in silicas show a linear behavior in the relaxation times that can be well described by an Arrhenius temperature equation:

$$\tau(T) = \tau\infty exp(Ea/RT) \qquad \text{(Equation 2)}$$

The values of the activation energies, T_g and the values of the pre-exponential factors, both of the processes in FNB constrained in silica and the alpha process in bulk FNB, are included in Table 5.

Table 4. Glass transition temperatures, activation energy and $\tau\infty$ values for native drug, FNB@MSNs and FNB@MSNs_APTES determined from dielectric data.

Sample	E_a (kJ/mol)	$\tau\infty$ (s)	T_g (°C) (τ = 100 s)
FNB@MSNs	118	6.31×10^{-25}	-39.1
FNB@MSNs _APTES	135	2.13×10^{-29}	-45.2
Bulk FNB	463	9.7×10^{-16}	-25.5

4. Release

The solution media for drug release was composed by phosphate buffer at pH 8 and ethanol in the w/w proportion of 90:10. Ethanol was chosen due to the higher solubility of FNB in

this medium than aqueous medium.[28] Base line was done with a quartz cuvette with 3 mL of the PBS:ethanol solution. Drug release was monitored during 8 hours by UV-Vis following the procedure developed in the laboratory.[29] The corresponding sample was added in a dialysis membrane with 200 µl of PBS/EtOH (10%) that was inserted in a quartz cuvette filled with 3.3 mL of the solution media (PBS/EtOH mix) and kept under continuous stirring at 400 r.p.m. Successive UV-Vis spectra (200 to 700 nm) was collected at an acquisition rate of 400 nm/min. During the first 4 hours, spectra was taken every 60 seconds and then, every 600 seconds until complete 8 hours. To analyse the release profile, absorbance at λ = 289 nm was represented as a function of time (figure 12). For both samples (APTES and TMPS functionalized MSNs), a gradual increase of the absorbance due to fenofibrate release is observed and there is no initial faster diffusion of FNB molecules from both composites indicating that mostly all the FNB molecules should be located deeper inside the silica pores.

Considering that very similar masses of both samples were put in the cuvette it can be concluded that the release from FNB@MSNs_APTES is faster than from FNB@MSNs_TMPS. To estimate the concentration of FNB a calibration curve was construct and results indicates a low release of fenofibrate in both composites as reported in table 5 (around 2.7 % in silica modified with APTES and less than 0.5 % in the one modified with TMPS).

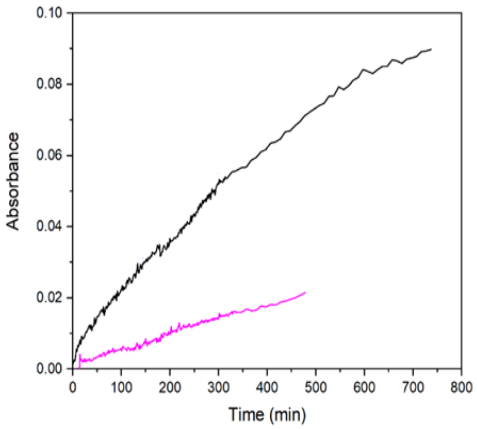

Figure 12. Release profile of FNB@MSNs_APTES (black line) and FNB@MSNs_TMPS (pink line) obtained at λ = 289 nm.

Table 5. FNB release after 8 hours

Sample	m_{MSNs} (g)[a]	n_{FNB} (mol)[b]	$n_{Released}$ (%)[c] (after 8h)
FNB@MSNs_APTES	1.73×10^{-3}	1.09×10^{-6}	2.7
FNB@MSNs_TMPS	1.63×10^{-3}	1.50×10^{-6}	0.4

[a] grams of MSNs, [b] number of moles of FNB in MSNs, [c] percentage of moles released after 8 hours (relative to loaded FNB).

5. Conclusions

Mesoporous silica nanoparticles (MSNs) with (49 ± 6.6) nm of external diameter and regular pores of 3 nm have been prepared. The external and internal surface of these MSNs was modified with organic alkoxysilanes containing functional groups with different polarity; hydrophilic 3-(Aminopropyl)triethoxysilane (APTES) and hydrophobic trimethoxy(phenyl)silane (TMPS). The modification was confirmed by FTIR and 1H NMR. Subsequently, fenofibrate (FNB), was loaded in the three different silicas (bare MSNs, MSNs_APTES and MSNs_TMPS) to achieve its amorphization and to control its release. FTIR spectra show that fenofibrate is clearly absorbed in the matrix and it interacts with the silica surface. A set of techniques, including calorimetry (DSC) and dielectric relaxation spectroscopy (DRS) were used to obtain detailed information on the physical state of the loaded FNB. DSC shows that full FNB amorphization was successfully achieved and the T_g was detected in the three composites at lower temperatures than the T_g of bulk FNB. Additionally, the temperature range in which the material undergoes a second order phase transition (i.e., liquid to glass or vice versa), is larger with respect to the one in native fenofibrate because of the interaction with the silica. The molecular mobility of the loaded drug was investigated by dielectric relaxation spectroscopy (DRS). By analyzing the dielectric modulus of fenofibrate no signal of melting is observed when FNB is loaded in mesoporous silica nanoparticles (in accordance with thermograms obtained by DSC), confirming that FNB is stabilized in its amorphous disordered state. Moreover, in FNB loaded in bare MSNs and MSNs_APTES samples, a dipolar mechanism is clearly observed, and it is shifted to higher temperatures/lower frequencies relatively to the α process (associated to the glass transition) of bulk FNB. The glass transition temperatures estimated

from dielectric data are significantly lower than the T_g determined by differential scanning calorimetry (DSC). This fact, together with the Arrhenius temperature dependence and a relatively low activation energy, suggests a surface process and not a true α relaxation (nevertheless more work must be done to fully confirm this hypothesis). Additionally, this relaxation mode is faster when FNB is loaded in MSNs_APTES than in bare MSNs, indicating that the presence of APTES induces weaker interactions with FNB. The release of FNB from the MSNs was followed by UV-Vis spectroscopy, showing that MSNs_APTES provide faster FNB release kinetics than MSNs_TMPS in a period of 8 h. The fact that the amount of FNB released form functionalized silicas is very low in the period of 8h, indicates that both systems are able to control the release process for a long period of time. In conclusion, by tuning the pore functionality of MSNs, it is possible to stabilize the amorphous state of the crystallizable drug fenofibrate, and also to modulate the drug release kinetics, to fit the desired applications.

6.Bibligraphy

[1] S. Baghel, H. Cathcart, N. J. O'Reilly. Solid Dispersions: A Review of Amorphization, Crystallization, Stabilization, Solid-State Characterization, and Aqueous Solubilization of Biopharmaceutical Classification System Class II Drugs, *Journal of Pharmaceutical Sciences*, 105 (9), 2527–2544, 2016.

[2] Savjani K.T, Gajjar A. K., Savjani J. K.. Drug Solubility: Importance and Enhancement Techniques. ISRN *Pharmaceutics Volume*, Article ID 195727, 2012.

[3] Amidon G. L., Lennernäs H., Shah V. P., Crison J. R. A theoretical basis for a biopharmaceutic drug classification: The correlation of in vitro drug product dissolution and in vivo bioavailability. *Pharmaceutical Research*, 12, 413–420, 1995.

[4] Grohganz H., Lobmann K., A Priemel P., Refining stability and dissolution rate of amorphous drug, *Pub Med expert opinion on drug delivery,* 11(6), 2014

[5] Beiner M., Pankaj S., Enke D., Steinhart M.; manipulating the crystalline state of pharmaceuticals by nanoconfinment, *Nano Lett,* 7, 5, 1381–1385, 2007.

[6] Graubner G., Anders N., Sonnenberger N., Steinhart M., morphology of porous host directs preferred polymorh formation and influences kinetics of solid/solid transition of confined pharmaceuticals, *Cryst. Growth Des.,* 14, 1, 78–86, 2014

[7] Narayan R., Nayak U. Y., Raichur A. M., Garg S. Mesoporous Silica Nanoparticles: A Comprehensive Review on Synthesis and Recent Advances. *Pharmaceutics*, 10, 118 (1-49), 2018.

[8] Chircov C., Spoiala A., Ficai D., Mesoporous silica platforms with potential application in release and adsorption of active agents, *Molecules*, 25(17), 3814, 2020.

[9] Kresge C. T., Leonowicz M. E., Roth W. J, Vartuli J. C., Beck J. S., Ordered mesoporous molecular sieves synthesized by a liquid-crystal template mechanism. *Nature*, 359, 710–712, 1992.

[10] Ribeiro T., Rodrigues A. S., Calderon S., Fidalgo A., Gonçalves J. L. M., André V., Duarte M. T., Ferreira P. J., Farinha J. P. S., Baleizão C., Silica nanocarriers with user-defined precise diameters by controlled template self-assembly, *Journal of Colloid and Interface Science*, 561, 609–619, 2020.

[11] Stober W., Fink A.,Bohn E., Controlled growth of Monodisoerse Silica spheres in the micron size range *Journal of Colloid and Interface* 26, 62–69, 1968.

12 Raman I., Padavettan V., Synyhesis of silica nanoparticles by sol-gel: size dependent properties, surface modification, and applications in silica polymer nanocomposites, *A review. Journal of nanomaterials*, 2012.

[13] Trewyn, B. G.; Slowing, I. I.; Giri, S.; Chen, H.; Lin, V. S.-Y. Synthesis and Functionalization of a Mesoporous Silica Nanoparticle Based on the Sol - Gel

Process and Applications in Controlled Release, *Acc. Chem. Res.,* 40 (9), 846–853, 2007.

[14] Dominik B., Post synthetic functionalization of mesoporous silica, *Nanoscale*, 2(6), 887–892, 2010.

[15] Lopes A. B. C.; Farinha J. P. S , Baleizao C., Smart nanoparticles for controlled release applications, Master Thesis, 2018.

[16] Slowing, I. I., Trewyn, B. G., and Lin, V. S. Y, Effect of surface functionalization of MCM-41-type mesoporous silica nanoparticles on the endocytosis by human cancer cells, *J. Am. Chem. Soc.*, 128(46), 14792–14793, 2006.

[17] Vallet-Regi M.,Tamanoi F. Mesoporous Silica-based Nanomaterials and Biomedical Applications, Part A, *The Enzymes,* 43,1–10, 2018.

[18] Blin J.L, Gérardin C., Rodehüser L., Selve C., Stébé M. J,. Influence of alkyl peptidoamines on the structure of functionalized mesoporous silica. Chemistry of Materials, 16(24), 5071–5080, 2004.

[19] She X., Chen L, Li C., He C, He L., Kong L. ,Functionalization of hollow mesoporous silica nanoparticles for improved 5-FU loading, research article. *Journal of nanomaterial*, volume, ID 872035, 2015.

[20] Coates J., interpretation of infrared spectra, a practical approach, *Encyclopedia of Analytical Chemistry: applications, theory and instrumentation,* pp.10815-10837,2000

[21] Arkles B., Larson G., Book: silicon compounds silanes & silicones, 3rd chapter infrared analysis of organosilicon compounds, pp.175-178,2013

[22] Crucho l. C., Beleizao C., Farinha J. P. S., Functional group coverage and conversion quantification in nanostructured silica by ^{1}H-NMR. *Anal. Chem.* 89(1), 681–687, 2016.

[23] Heinz A., Gordon K. C., McGoverin C. M., Rades T., Strachan C. J., Understanding the solid-state forms of fenofibrate – A spectroscopic and computational study., *European Journal of Pharmaceutics and Biopharmaceutics* 71, 100–108, 2009.

[24] Diogo H. P., Viciosa M. T., Moura Ramos J. J. ,Differential scanning calorimetry and thermally stimulated depolarization currents study on the molecular dynamics in amorphous fenofibrate. *Thermochimica Acta,* 623, 29–35, 2016.

[25] Alhalaweha A., Alzghoulb A., Mahlina D., Bergströma C. A. S., Physical stability of drugs after storage above and below the glass transition temperature: Relationship to glass-forming ability. *Int. Journal of Pharmaceutical,* 495, 312-317, 2015.

[26] Sailaja U., Thayyil M. S., Kumar N. S. K., Govindaraj G., Molecular dynamics of amorphous pharmaceutical fenofibrate studied by broadband dielectric spectroscopy., *Journal of Pharmaceutical Analysis,* 6(3), 165–170, 2016.

[27] Fulcher G.S., Analysis of Recent Measurements of the Viscosity of Glasses. J. Am. Ceram. Soc., 8, 339–355, 1925.

[28] Watterson S., Hudson S., Svard M. ,Rasmuson A.C., Thermodynamics of Fenofibrate and Solubility in Pure Organic Solvents, Fluid Phase *Equilibria*, 367, 143–150, 2014.

[29] Gonçalves J. L., Crucho C.I., Alves S. P. C., Baleizão C., Farinha J. P. S. ,Hybrid Mesoporous Nanoparticles for pH-Actuated Controlled Release, Nanomaterials, 9(3), 483, 2019.